Oil & Natural Gas Technology

DOE Award No.: DE-FE 0009963

Quarterly Research Performance Progress Report (Period ending 06/30/2014)

Measurement and Interpretation of Seismic Velocities and Attenuations in Hydrate-Bearing Sediments

Project Period (10/1/2012 to 9/30/2015)

Submitted by:
PI: Michael Batzle
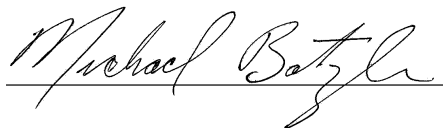Colorado School of Mines
DUNS #010628170.
1500 Illinois Street
Golden. CO 80401
e-mail: mbatzle@mines.edu
Phone number: (303) 384-2067
Submission Date: 8/4/2014

Prepared for:
United States Department of Energy

National Energy Technology Laboratory

Office of Fossil Energy

Abstract:

Measurement and Interpretation of Seismic Velocities and Attenuations
in Hydrate-Bearing Sediments

Grant/Cooperative Agreement DE-FE 0009963.

We continue to make good progress on this project to measure the seismic velocity and attenuation in methane hydrate-bearing sediments. Modifications and upgrades to laboratory equipment are largely complete and measurements are underway. For this reporting period we focused on acquisition techniques, data evaluation as well as extending the capabilities of our imaging equipment.

- The cooling and pressure systems have been installed in the CT scanner and are now undergoing tests.

- The low frequency system phase measurements (used to calculate attenuation) are being analyzed and extended

- In situ (well log) data is now being collated and examined to derive velocity and attenuation for comparison to our laboratory measurements.

 process more accurate and robust. Formation of hydrates in the Bentheim sandstone are heterogeneous. Velocities are roughly consistent with a combination of the pore-filling and envelope-cementing models.

Contents:

Figures:

Executive Summary:

Improving hydrate saturation estimates from geophysical measurements such as seismic surveys require more information than just velocity-saturation relationships. Seismic attenuation has been demonstrated to be directly related to the hydrate content of sediments. However, the magnitude and mechanisms of this attenuation are still poorly understood. This project to measure seismic velocities and attenuations under known saturations and textural conditions is well underway.

During this last reporting period, an x-ray transparent vessel has been built and tested for image quality as well as for long-term temperature and pressure stability. The vessel needed to be cooled to reach the hydrate stability region without interfering with the scanning mechanism. A chilled air flow system was installed and final adjustments are being made to regulate the temperature. Scanner parameters still must be adjusted to produce the highest resolution images.

Equipment has been upgraded and sample strain data is collected under a broad range of frequencies. The amplitudes and phases allow velocities and attenuations to be calculated. However, noise and errors can be large. The new system can overcome this problem by both a more dense sampling and direct measurement of the signal standard deviation. Spurious points can be identified and removed to increase the signal quality substantially. Fortunately, measurements within the pressure vessel have even higher quality due to the increased effective shielding.

In situ log data has been provided to this project to compare with our laboratory data. For the Mount Elbert well, two prominent hydrate zones (zones "C" and "D") can be used to test our results. The reported hydrate saturations were calculated using a variety of log measurements. Nuclear Magnetic Resonance (NMR) measurements in combination with other tools are considered to provide the most accurate estimates. Models of compressional and shear velocities were developed by other authors to match the saturations from the NMR logs. We are developing similar empirical and theoretical relationships based on compressional and shear wave attenuations extracted from the full waveforms.

Accomplishments

A. CT cooling System

To grow hydrates within the CT scanner, both temperatures and pressures need to be control to keep the environment within the hydrate stability field. Pressures are controlled by Isco digital pumps and contained within the torlon vessel, as described in the previous period report. Our initial procedure to inflict low temperatures will consist of chilled air flow on the vessel. Other facilities have employed circulating chilled confining pressure or Peltier plates. These systems are more complex, requiring separate pumps or heat sinks, and could interfere with the motion of the scanner base. Care needed to be taken to remove any moisture from the cooling air stream. At lower temperatures, moisture would condense within the flow.
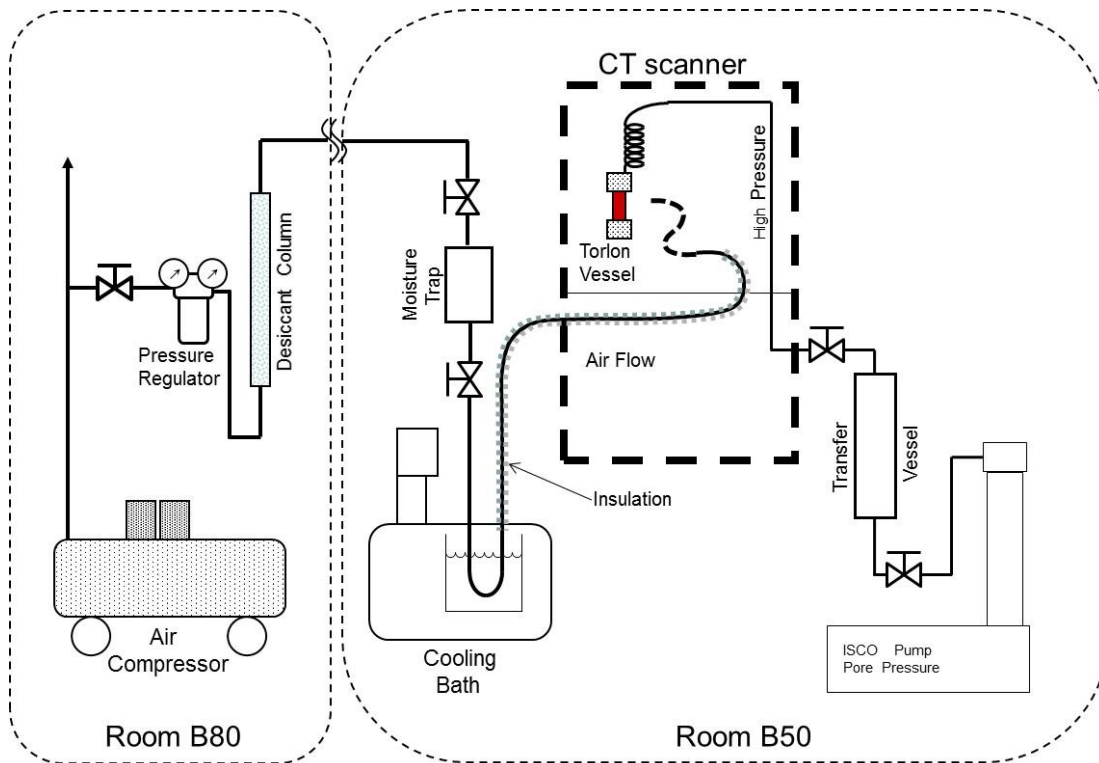
Figure 1: Schematic of the flow system to cool the Pressure vessel within the CT scanner

A calibration column consisting of F110 Ottawa sand, 1mm glass beads, and Fox Hills Sandstone was assembled to test the sensitivity of the CT scan resolution to various scanning parameters within the pressure vessel. This column alongside the vessel is shown in Figure 2.
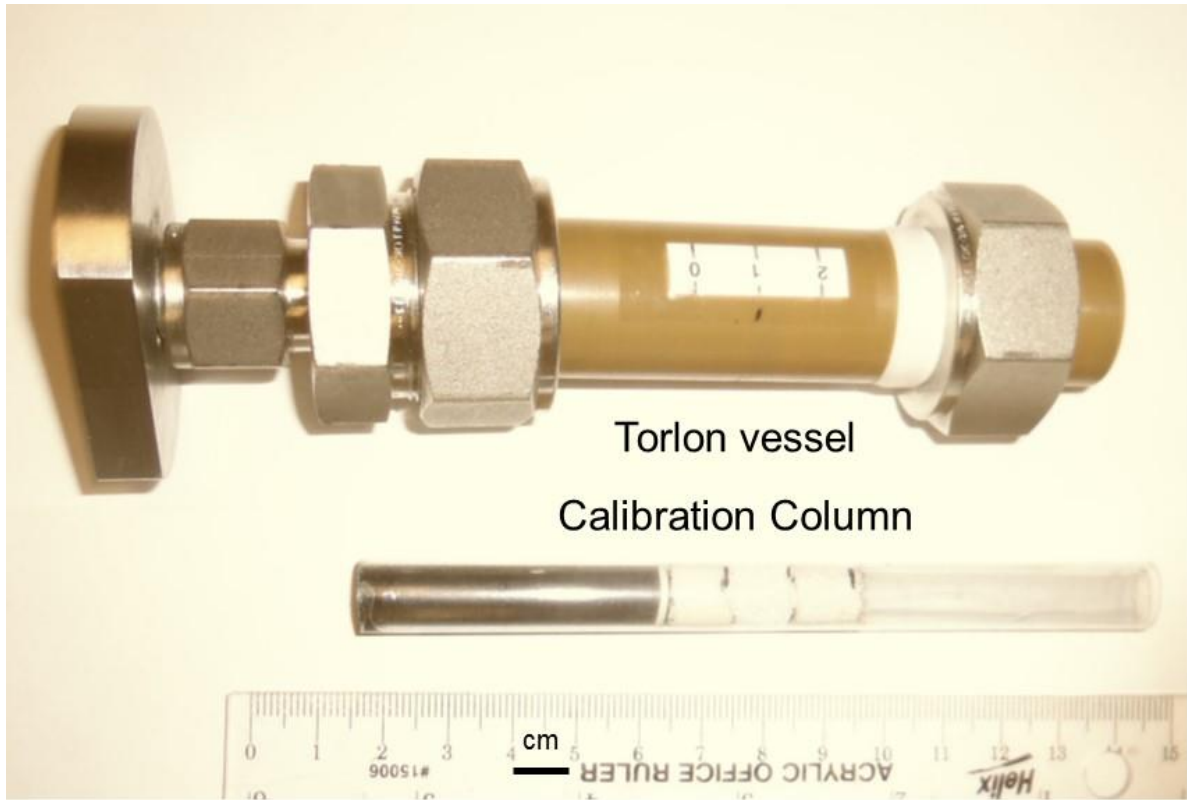
Figure 2. Calibration column outside the torlon vessel.

In Figure 3, the vessel installed in the CT scanner is seen. What is not shown is the additional thermal jacketing around the vessel. We want to keep the system as simple as possible, which justifies the air cooling system. Otherwise, electronic cables and pressure tubes still need to be attached to the vessel. These are shown at the top of Figure 3. These connections must not interfere with the motion of the vessel.
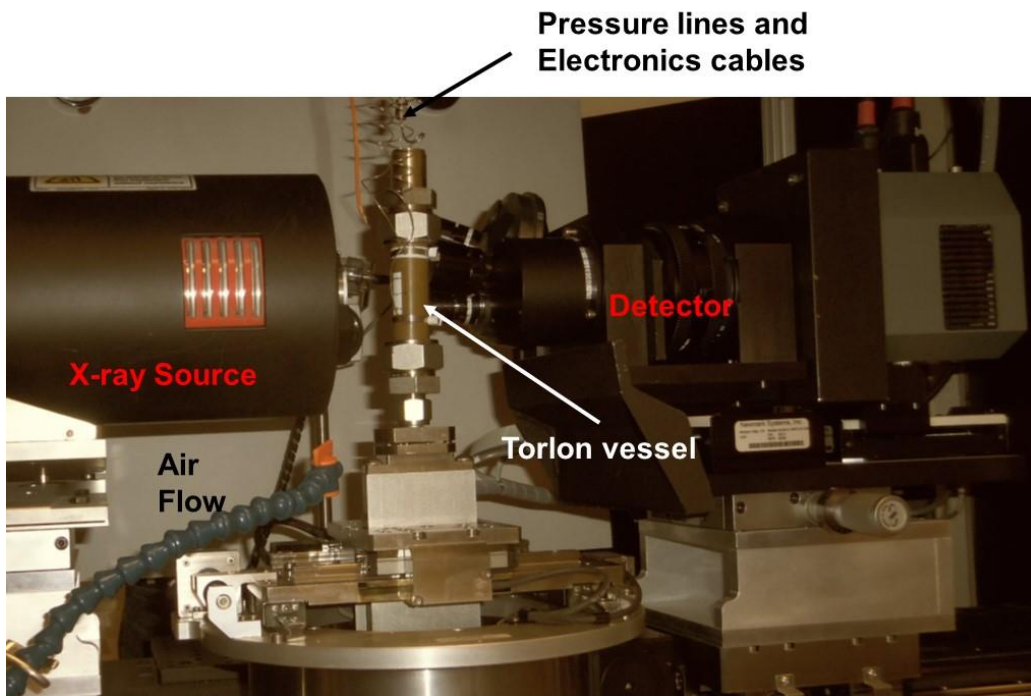
Figure 3. Pressure vessel inside CT scanner (vessel insulation removed)

Preliminary scans of the calibration column within the Torlon vessel are shown in Figure 4. Tests on other vessels we have manufactured indicate that the vessel walls can be made even thinner, without loss of pressure capability. We are now focusing on optimizing the scan parameters to optimize the resolution within the sample.
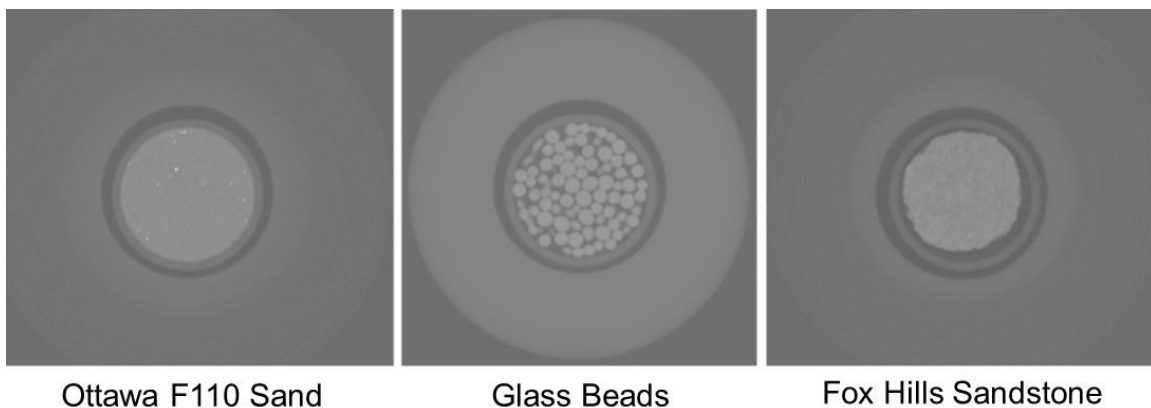
Figure 4. CT scans of the calibration column materials within the torlon vessel.

B. Calibration of Low Frequency System:

The low frequency system measures the amplitude and phase of deformation of a sample using strain gages. The sample is in line with an aluminum standard and direct comparison with the aluminum eliminates much of the noise. An example of the acquired data is shown in Figure 5. For each gage pair, or channel, both amplitude and phase are measured. In reality, at each specific frequency three measurement cycles are made. The reported values are the average amplitudes and phases. Since three set of data are collected, the procedure also allows us to calculate the standard deviation (SD) of these values. This SD gives us a straight forward method to ascertain the quality of any given data point.

Operator PR
Sample# PEEKRoomT4
5/9/2013 4:10:48 PM

	Chan 1	Chan 2	Chan 3	Chan 4	Chan 5	Chan 6	Chan 7	Chan 8	Chan 9	Chan 10	Chan 11	Chan 12
Gain	1000	1000	1000	1000	1000	1000	1000	1000	1000	1000	1000	1000
Guage Factor	155	155	2	0	2	155	155	2.11	2.11	0	0	0

Notes
Sample Info: PEEK test, room temperature, outside vessel
Confining Pressure: 0 psi
Pore Pressure: 0 psi
Temperature: room °C
Pore Fluid: none
Bridge Voltage: 12
Other Notes: PEEK test, room temperature, outside vessel

Freq	Amp	Chan 1 Ampl. Average	Chan 1 Ampl. Std Deviation	Chan 1 Phase Average	Chan 1 Phase Std Deviation	Chan 2 Ampl. Average	Chan 2 Ampl. Std Deviation	Chan 2 Phase Average	Chan 2 Phase Std Deviation	Chan 3 Ampl. Average	Chan 3 Ampl. Std Deviation	Chan 3 Phase Average	Chan 3 Phase Std Deviation
30	0.15	0.03712951	0.00003065	4.47504951	0.19420293	0.03519125	0.00002067	4.43148507	0.16440304	0.00272391	0.00002232	-175.5659137	2.47385016
38.42049669	0.15	0.03707819	0.00000718	2.80426294	0.2525681	0.03511839	0.0000192	2.68674142	0.09645746	0.00274229	0.00003018	182.2747481	0.33844219
49.20448553	0.15	0.0369875	0.00002167	1.20247585	0.20470043	0.03499483	0.00000993	1.27585371	0.21664764	0.00271409	0.00002818	181.6244617	2.03364709
63.01535911	0.15	0.03698968	0.00109162	1.58925436	6.73088639	0.03500514	0.00087452	1.24777399	5.59912027	0.00275132	0.00031624	-170.7785828	20.70725344
80.7027132	0.15	0.03667654	0.00001189	-1.70673848	0.18042573	0.0347289	0.0000113	-1.4921541	0.1849751	0.00267565	0.00002779	-179.3741671	2.07263355
103.3546108	0.15	0.03652755	0.00005341	-3.92874636	1.26943434	0.03453573	0.00009346	-4.67506805	2.2018434	0.0027119	0.00004026	177.9500435	2.69083437
132.3645161	0.15	0.03641868	0.00097766	2.27878045	13.79394054	0.03457828	0.00153018	7.26270987	19.74281201	0.0026491	0.0000218	-183.9983481	2.72343797
169.5170151	0.15	0.03607517	0.0001277	-6.07314062	5.10726164	0.03418511	0.00003765	-9.24463828	0.38351492	0.00252886	0.00002715	-179.467764	1.59829447
217.0975973	0.15	0.03573398	0.00005785	-9.68366593	0.4568775	0.03370538	0.00004451	-9.97442409	0.59663002	0.00264551	0.00005121	-190.6990924	4.05600763
278.0332506	0.15	0.03546089	0.00007734	-12.94584715	0.87713584	0.03341959	0.00007189	-13.02336343	1.29578202	0.00261086	0.00012858	160.3907851	13.64857762
356.0725194	0.15	0.03542564	0.00006579	-15.94913952	0.58566245	0.03320809	0.00007593	-16.18262541	0.30889879	0.00257043	0.00009109	-190.7603144	2.78006566
456.0161018	0.15	0.03518471	0.000016	-20.15421256	0.41099601	0.03253033	0.0000262	-20.41716265	0.07615284	0.00257938	0.00006781	161.7722943	4.01474725
584.0121709	0.15	0.03620681	0.00004149	-23.12321884	0.22828434	0.0333094	0.00004462	-23.21529192	0.34843613	0.00262157	0.00002386	-198.5969226	3.49843419
747.9345893	0.15	0.03830007	0.00007836	-29.27520561	0.40605111	0.03462764	0.00007059	-29.16489798	0.20636948	0.00274326	0.00007329	153.8645981	3.41364562
957.8672804	0.15	0.04398251	0.00001605	-40.74302328	0.19232185	0.04488155	0.00005771	-30.82721333	0.17638319	0.00289035	0.00004473	-222.7032702	2.12413768
1226.724556	0.15	0.09307374	0.00002887	-46.33549593	0.09325132	0.08062118	0.00005804	-46.23610118	0.23895591	0.00604271	0.00004172	135.4565535	1.9948704
1571.045558	0.15	0.02081455	0.00007473	234.1977267	0.10169603	0.01356285	0.00002954	-131.0788782	0.27022569	0.0010935	0.00003133	64.27509587	10.60194217
2012.011688	0.15	0.05161036	0.00003694	-225.8162016	0.15194779	0.03534487	0.00008747	135.006779	0.39541473	0.00285901	0.00002321	-47.75716164	2.90317376
2576.749614	0.15	0.00467319	0.00024587	-173.7261545	40.97970986	0.00618138	0.000019	264.5434094	1.4984317	0.00057596	0.00007047	-227.9224237	19.46674263
3300	0.15	0.00929715	0.0000135	123.6771995	0.99577889	0.00597616	0.00004776	29.33972153	141.3077984	0.00055649	0.00005429	-253.4796406	166.8775725

Figure 5. Example data sheet for the low frequency measurements. Note that standard deviations are collected along with the measurements of amplitude and phase.

As described previously, the experimental procedure we use is an extensional stress-strain measurement. If the assumption of isotropic, homogeneous materials is valid, then we need collect only two independent elastic parameters. In our apparatus, we do not measure displacement (as do most other experimental setups) but the strain on the sample surface. The axial strain, ε_{33}, under our boundary conditions is given by

$$\varepsilon_{33} = \frac{\partial u}{\partial x} = F\cos\left(\sqrt{\rho/E} \times \omega x\right)\sin(\omega t) \ , \tag{1}$$

where u is displacement, x is location, ω is frequency, ρ and E are density and Young's modulus respectively, and F is an elastic constant defined by the geometry. From the horizontal strain we can extract Poisson's ratio, ν, where the superscript '*rx*' refers to the rock value.

$$\nu^{rx} = -\frac{\varepsilon_{11}^{rx}}{\varepsilon_{33}^{rx}} \ . \tag{2}$$

Axial strain measurements are also made on the aluminum standard (superscript '*al*'), and the rock's Young's modulus, E^{rx} is derived from the known Young's modulus of aluminum, E^{al}, and the ratio of the aluminum to rock strain:

$$E^{rx} = E^{al}\frac{\varepsilon_{33}^{al}}{\varepsilon_{33}^{rx}} \ . \tag{3}$$

Well-known relationships now can be used to calculate all of the remaining elastic properties for an isotopic homogeneous sample.

$$\mu = \frac{E}{2(1+\nu)} \ . \tag{4}$$

$$K = \frac{E}{3(1-2\nu)} \ . \tag{5}$$

$$V_S = \sqrt{\mu/\rho} \ . \tag{6}$$

$$V_P = \sqrt{(K + \tfrac{4}{3}\mu)/\rho} \ . \tag{7}$$

Here μ and K are the shear and bulk moduli, and Vs and Vp are the shear and compressional velocity.

In an anelastic material, the deformation will lag in time from the applied stress. For a sinusoidal applied stress, this phase lag (θ) can be described in terms of the complex modulus

$$M^* = \text{Re}[M] + i\,\text{Im}[M] \tag{8}$$

Then, attenuation (1/Q) can be defined as

11

$$Q^{-1} = Im[M] / Re[M] \tag{9}$$

$$\text{and } Im[M] \ Re[M] = \tan \theta \approx \theta. \tag{10}$$

To obtain the shear-wave attenuation we use the following relation (White, 1965):

$$1/Q_S \simeq [(1 + \nu) / Q_E - \nu \tan \theta_v] / (1 + \nu) \tag{11}$$

where θ_v is the phase lag between the vertical and horizontal strain on the rock sample. Poisson's ratio at seismic frequencies is obtained from the ratio of the horizontal and vertical strain amplitude on the rock. We then estimate the P-wave and the bulk compressibility attenuation from the relations derived by Winkler and Nur (1982):

$$(1 - \nu)(1 - 2\nu) / Q_P = (1 + \nu)/Q_E - 2\nu(2 - \nu) / Q_S \tag{12}$$

$$(1 - 2\nu) / Q_K = 3 / Q_E - 2(\nu + 1) / Q_S \tag{13}$$

Errors and Noise

When the environment is noisy or the signals have small amplitude, then the errors in estimating either amplitude or phase become large. This translates into large errors in the derivation of moduli and velocities as well as attenuations. The noise depends on several factors including system shielding. The results are also frequency dependent. Figure 6 shows example results for measurements both outside and inside the large pressure vessel. On bench top, or outside the pressure vessel (black points), large noise spikes are seen, particularly at low frequencies. Much of this noise is associated with building equipment (fans, pumps) running nearby. Note also the increased noise at 120 Hz. This is not unexpected, and results from an overtone of standard power.

The good news is that we collect the data with the assembly inside the pressure vessel. This large mass of steel provides an excellent shield and filters out much of the noise. The improvement inside the vessel (blue points) is obvious.

Similar observations can be made of thephase measurements. In the example shown in Figure 7, strong noise spikes are seen at 120 Hz and 240 Hz. Again, overtones of our 60 Hz power supply.
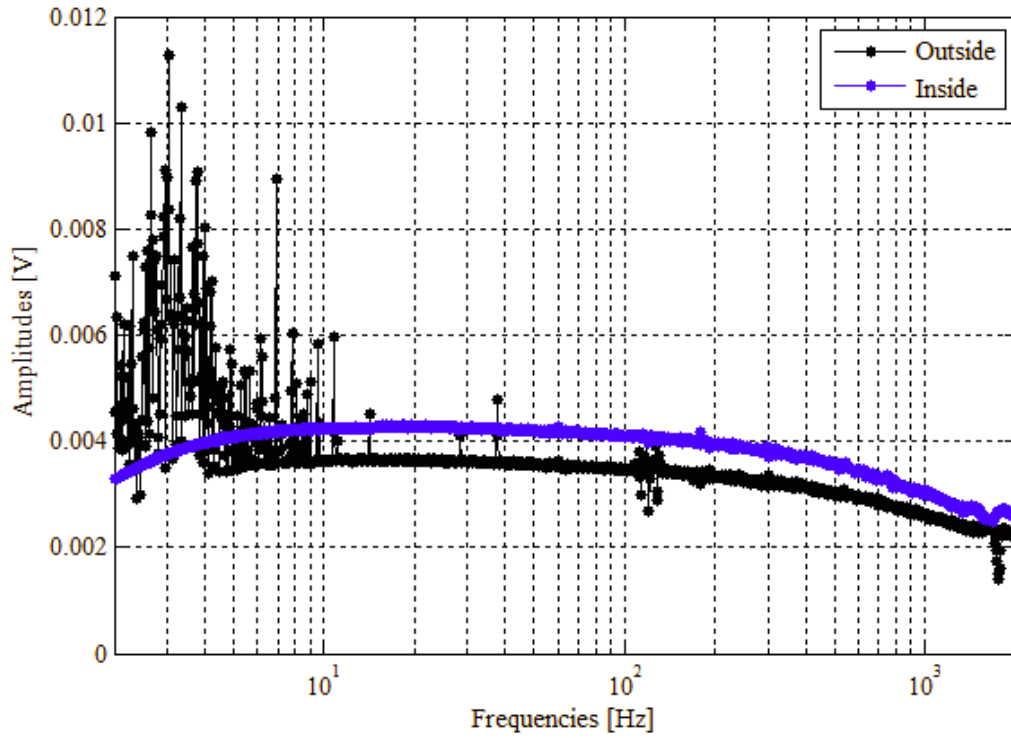
Figure 6. Amplitude of strain signals on a calibration standard collected both 'bench top' or exposed (black), and collected with the assembly inside the pressure vessel (blue). The pressure vessel provides shielding and substantially reduces noise.
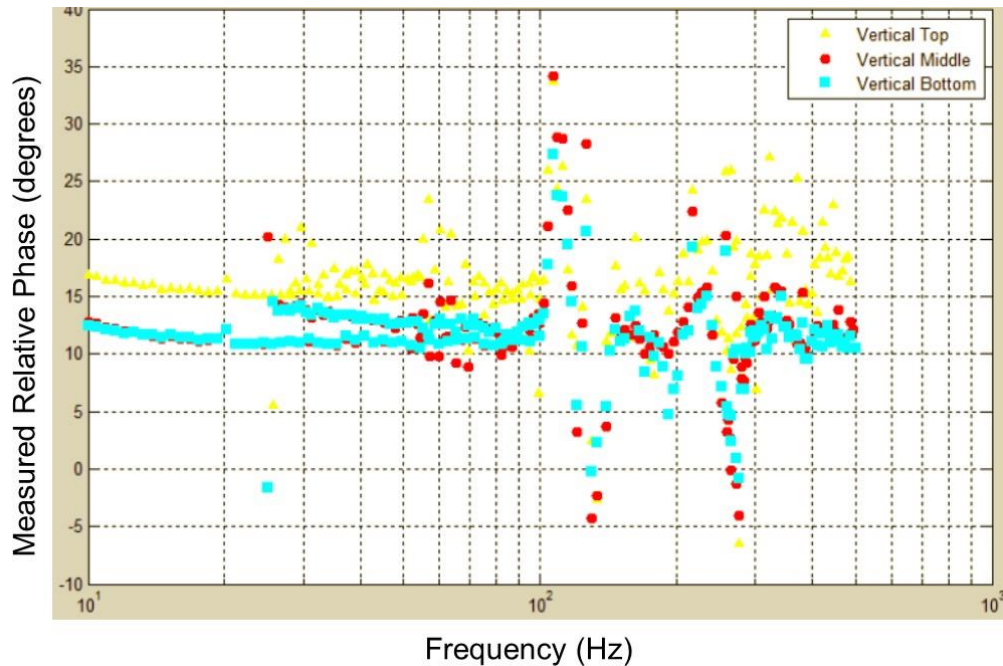
Figure 7. Phase measurements on a PEEK sample. Note the influence of noise or a system resonance at about 120 and 240 Hz (overtones of 60 Hz)

C. *In situ (well Log) data:*

Much of the data we use for comparison will be from the Mallik, Mount Elbert, and Ignik Sikumi wells. This data already has been provided to us by Tim Collett of the USGS. Guerin and Goldberg (2002, 2005) have already examined some of these data and extracted attenuation estimates. An excellent starting point for us.

Data from the Mount Elbert well is shown in Figure 8. This simple plot shows the sand-rich zones starting at 2015 and 2135 feet (track 1). High hydrate saturation can be inferred immediately from the strong resistivity (track 2) and sonic (track 3) response.
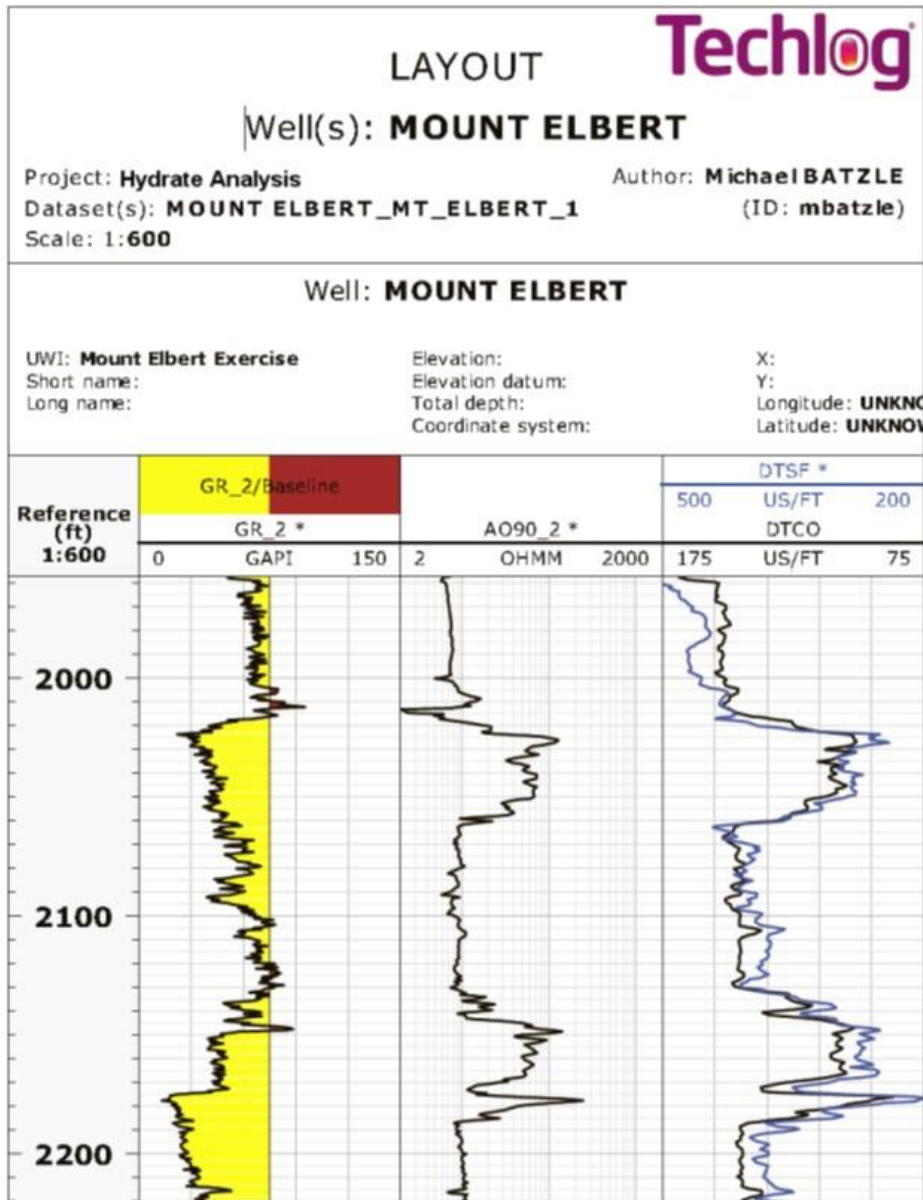
Figure 8: Gamma ray (GR), Resistivity (AO90), and Sonic (compressional – DTCO; and fast shear - DTSF) for the two prominent hydrate zones in the Mount Elbert well, Alaska. Data provided by Schlumberger.

The sensitivity of Nuclear Magnetic Resonance measurements (NMR) to free water makes the NMR log (here CMR) another valuable tool to quantify hydrate content (Figure 9). Collett and co-workers used these data, combined with other logs, to provide what they consider the most accurate estimate of hydrate saturation.

Lee and Collett (2011) use a composite poroelastic model to derive a similar hydrate saturation estimate from sonic logs (Figure 10). For exploration data sets, such detaied calibration is not possible. Velocity data (either from moveout analysis or inversions) is not sufficient. We are now working on extracting attenuation-related parameters from the in situ data. These results will be compared and calibrated against our laboratory measurements.
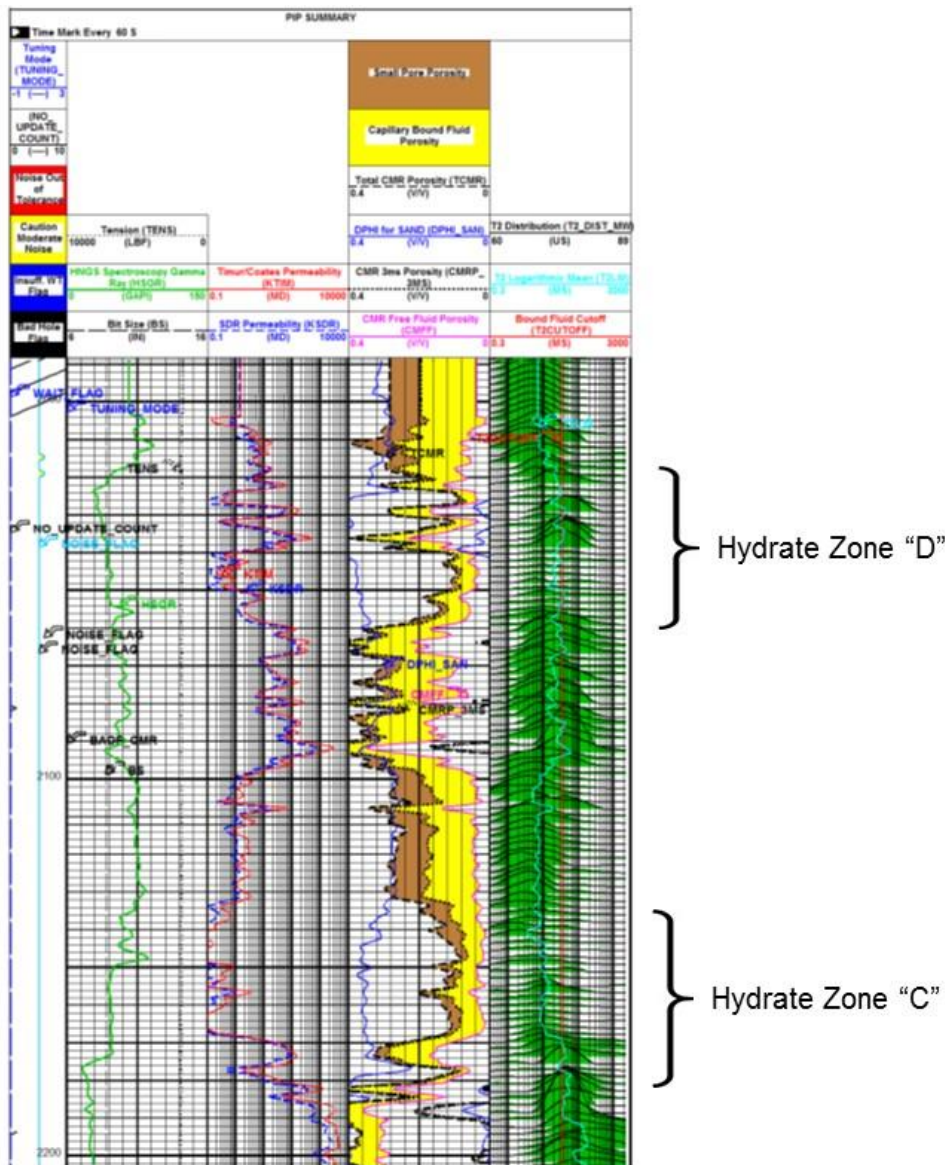

Figure 9: Magnetic Resonance log (CMR) in the Mount Elbert well used to identify the zones of high hydrate saturation. Data provided by Schlumberger and T. Collett.
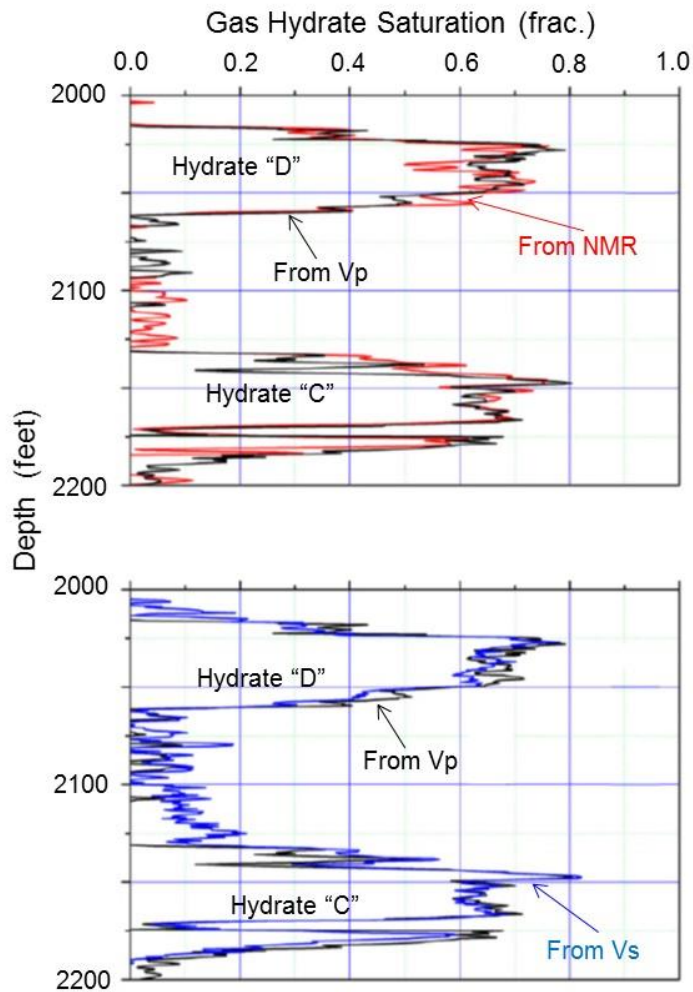
Figure 10: Estimated gas hydrate saturation in the Mount Elbert well using NMR (CMR), compressional wave speed (Vp), and shear wave speed (Vs).

Plans

During the next period, we will largely focus on the three topics described in this quarterly report:

- Growth of hydrates within the CT scanner and documenting their textures.

- Further measurements of velocity and attenuation, particularly broadband measurements using the Low Frequency device. We will complete the measurements on the pure hydrate phases.

- Attenuation estimates derived from full-waveform sonic logs using data provided by Tim Collett.

Methane hydrate powder can be produced using the excess methane-ice conversion. However, to make velocity and attenuation measurements on the pure material, we must compact the powder into a (near) zero porosity polycrystalline pellet. The technique of Durham et al. 2001 will be used first.

Experience has demonstrated that both velocities and attenuations will be strongly dependent on any unconverted water phase remaining in the sample. To assess the amount of water in our test samples we plan to make extensive use of the Nuclear Magnetic Resonance (NMR) system available in the petroleum engineering laboratory.

We will continue our efforts to grow methane hydrates out of methane in solution in water, but I expect only slow progress in that direction.

Since both graduate students working on this project have comprehensive exams due by the end of this year, I expect a good deal of productivity from both (nothing like a good deadline to motivate activity)

Participants and Collaborating Organizations

Name: George Radziszewski
Project Role: Research Faculty
Nearest person month worked this period: 1.5
Contribution to Project: Dr. Radziszewski spent his time establishing standards and procedures for running the MicroCT scanner .
Funding Support: "Organics, Clays, Sands and Shales (OCLASSH) consortium
Collaborated with individual in foreign country: No
Country(ies) of foreign collaborator: N/A
Travelled to foreign country: Yes
If traveled to foreign country(ies): (Poland)
Duration of stay: 3 weeks

Name: Mathias Pohl
Project Role: Graduate Student
Nearest person month worked this period: 3
Contribution to Project: Mr. Pohl prepared samples and collected ultrasonic data.
Additional Funding Support: N/A
Collaborated with individual in foreign country: No

Country(ies) of foreign collaborator: N/A
Travelled to foreign country: No
If traveled to foreign country(ies)
duration of stay: N/A

Name: Mandy Schindler
Project Role: Graduate Student
Nearest person month worked this period: 3
Contribution to Project: Ms Schindler prepared samples and collected CT data.
Additional Funding Support: N/A
Collaborated with individual in foreign country: No
Country(ies) of foreign collaborator: N/A
Travelled to foreign country: No
If traveled to foreign country(ies), (Germany, China)
duration of stay: 2 weeks

Name: Weiping Wang
Project Role: Laboratory Manager
Nearest person month worked this period: 1
Contribution to Project: Mr. Wang assisted in equipment fabrication
Additional Funding Support: Fluids consortium, Chinese Mining University
Collaborated with individual in foreign country: No
Country(ies) of foreign collaborator: N/A
Travelled to foreign country: Yes
If traveled to foreign country(ies), China
duration of stay: 3 weeks

Name: Andrew Markey
Project Role: Student
Nearest person month worked this period: 0 (just started)
Contribution to Project: Andrew will help collect CT data.
Additional Funding Support: 'Fluids' consortium
Collaborated with individual in foreign country: No
Country(ies) of foreign collaborator: N/A
Travelled to foreign country: No
If traveled to foreign country(ies),
duration of stay: N/A

Name: Michael Batzle
Project Role: Principle Investigator
Nearest person month worked: 1
Contribution to Project: Overall (dis)organization.
Funding Support: Academic faculty
Collaborated with individual in foreign country: No
Country(ies) of foreign collaborator: N/A
Travelled to foreign country: N/A

If traveled to foreign country(ies):

External Collaborations:
Dr. Tim Collett
US Geologic Survey
Denver, Colorado: (if foreign location list country)
Support: Data and guidance on interpretation and application
Tim continues to publish numerous papers on hydrate properties

Changes / Problems

The primary change is that George Radiziszewisky plans to retire at the end of this year. He has been responsible for much of the CT imaging conducted on our hydrate-bearing sediments. Half of George's full-time salary was contributed to this project as our cost share. We will replace him with Mr. Weiping Wang, our laboratory manager, with assistance from a student, Andrew Markey, who is proving adept at both running the CT equipment, and processing the images.

Special Reporting Requirements

None

Budgetary Information

Attached separately

References

Durham, W.B., Stern, L.A., and Kirby, S.H., 2003, Ductile flow of Methane hydrate, Can. J. Phys. 81, 373-380.

Guerin, G. and Goldberg, D., 2002, Sonic waveform attenuation in gas hydrate-bearing sediments from the Mallik 2L-38 research well, Mackenzie Delta, Canada, J. Geophys. Res. 107, EPM 1-11.

Guerin, G. and Goldberg, D., 2005, Modeling of acoustic wave dissipation in gas hydrate–bearing sediments; Geochem., Geophys., Geosyst. 6, Q07010.

Lee, M.W., andCollett, T.S., 2011, In-situ gas hydrate saturationestimated from various well logs at the Mount Elbert Gas Hydrate Stratigraphic Test Well, Alaska North Slope.

White, J. E., 1965, Seismic waves; radiation, transmission, and attenuation: McGraw-Hill, NewYork.

Winkler, K.W., and Nur, A., 1982, Seismic attenuation: Effects of pore fluids and frictional-sliding: Geophysics, 47, no. 1, 1–15.

Milestone Status

Our current position on the time chart is shown in Figure 11. We have approached the halfway mark of the project, and we are basically on schedule.
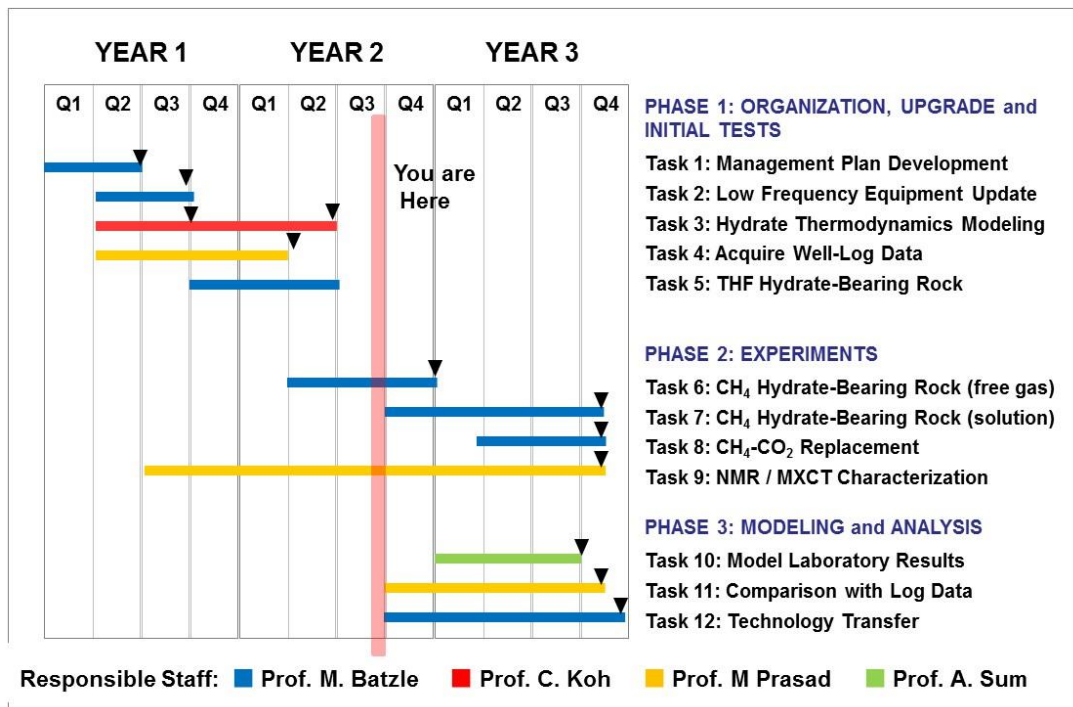

Figure 11. Milestone Status. We are at the end of our seventh quarter and are approaching the start of the final phase of this project.

Table 1. Milestone status

Measurement and Interpretation of Seismic Velocities and Attenuations in Hydrate-Bearing Sediments
DOE Award No.: DE-FE 0009963

Milestone Title / Description		Status	Completion date (completed or expected)
Completed:			
1	Project Management Plan (PMP)	Complete & approv..	1 Dec 2012
2	Modifications to low frequency system	Completed	1 Jun 2013
3	Modeling established using EOS	Completed	31 May 2014
4	Property models of hydrates completed	Completed	31 May 2014
5	Logs acquired and database estab.	Completed	15 Jun 2014
6	THF hydrate grown in pressure vessel	Completed	15 Apr 2014
Continuing or Planned			
7	Methane hydrates from free gas phase	Continuing*	31 Dec 2014
8	Methane hydrates from gas in solution	Planned	30 Jun 2015
9	CO2 replacing methane in hydrates	Planned	30 Sep 2015
10	MXCT scans conducted	Continuing*	30 Sep 2015
11	Effective media models complete	Planned	30 Sep 2015
12	Comparison to in situ data complete	Planned	15 Oct 2015
13	Information Dissemination	Continuing*	31 Dec 2015

*initial stages were completed on schedule, but the process continues throughout the project